X-Ray Lasing by Optical-Field-Induced Ionization

Peter Amendt, David C. Eder, and Scott C. Wilks
Lawrence Livermore National Laboratory, University of California, P.O. Box 808, Livermore, California 94550
(Received 11 February 1991)

A scheme for accomplishing tabletop x-ray lasing in Li-like Ne at 98 Å in an optically ionized plasma during recombination in the transient regime is presented. Saturation effects and parametric heating processes by stimulated Raman scattering are analyzed and found to allow energy efficiencies in excess of 10^{-5} for a 100-fsec-duration, 0.25-μm laser driver of intensity 10^{17} W/cm^2. Significant improvement in efficiency is indicated for shorter laser pulse lengths.

PACS numbers: 32.80.Rm, 42.55.Vc, 52.40.Nk, 52.50.Jm

The immediate prospect of short-pulse ($\tau \leq 100$ fsec), high-intensity ($I \geq 10^{17}$ W/cm^2), short-wavelength ($\lambda \sim 0.25$ μm) lasers[1] makes timely a further study of their use as drivers for x-ray lasers.[2,3] A major direction of research is the development of a tabletop version of an x-ray laser as an alternative to those presently driven by large and expensive inertial-confinement-fusion-class lasers.[4] Current x-ray lasers reach the desired ionization state through collisions with free electrons that are heated by an optical driver. Recent advances in short-pulse, high-intensity laser technology now admits the possibility of optically ionizing the plasma medium to the desired configuration with minimal heating of the ambient electrons.[1] Provided the postpulse electron temperature is sufficiently low, a rapid recombination cascade of electrons to the ground state of a chosen ion species can occur and lead to significant population inversion. The time scale of this initial inversion phenomenon is on the order of a radiative time for ground-state transitions ($3 \rightarrow 2$ in Li-like or $2 \rightarrow 1$ in H-like ions), which defines the transient regime of recombination lasing. This inversion episode is not to be confused with quasistatic recombination schemes which are characterized by time scales exceeding a hydrodynamic expansion or cooling time and by longer wavelengths characteristic of excited-state transitions ($4 \rightarrow 3$ in Li-like or $3 \rightarrow 2$ in H-like ions).[5]

The idea of achieving x-ray lasing in the transient regime has recently been addressed by Burnett and Enright[2] and Keane *et al.*[3] in a study of possible population inversions. There are several issues which may determine the experimental feasibility of this scheme: (1) saturation phenomena associated with potentially robust gains, (2) parametric heating mechanisms which may excessively heat the ambient electrons, and (3) possible energy efficiencies. By carefully addressing these issues in this Letter, we show that x-ray lasing in the transient regime is a practical experimental endeavor. In addition, we assess what optimal efficiencies are possible in tabletop x-ray lasers over the near term.

A promising candidate for an efficient optical-field-induced (OFI) ionization x-ray laser in the transient regime is Li-like Ne with its relatively low value of required laser intensity I_{req} ($\sim 10^{17}$ W/cm^2).[6] We begin our study of Li-like Ne with a simplified atomic kinetics description. There are three principle time scales: (1) the time scale for Saha equilibration of the upper states ($n>4$) following the ionizing pulse, which is assumed instantaneous (<100 fsec); (2) the transient lasing or radiative ($3 \rightarrow 2$) time scale which is our primary interest (~ 1 psec); and (3) the quasistatic recombination time scale (>100 psec). The number of Rydberg levels in Li-like Ne is determined by continuum lowering,[7] giving an uppermost level of $n \cong 13$. Since the $n=3$ to $n=2$ resonance transition (at 88 Å, shell averaged) is our main focus, the upper Rydberg states beyond about $n=7$ are not important beyond determining the He-like Ne population for a given electron density. For $n,l \rightarrow n',l'$ electron collisional-induced transitions, we use Coulomb-Born exchange collision rates when $n,n' \leq 5$;[8] otherwise, the semiempirical formulas of Sampson and Zhang are used.[9] The resulting detailed atomic model is then shell averaged to obtain a hydrogenic model.

Defining an initial time ($t=0$) as the instant following passage of the ionizing laser pulse we proceed to solve the rate equations for the level populations with the $n=2$–5 levels initially empty. Figure 1 shows the statistically weighted populations for these four lowest levels along with the $4 \rightarrow 3$ and $3 \rightarrow 2$ gain profiles after allowing for He-like ion depletion. We note that the $n=5$ level reaches Saha equilibrium in approximately 100 fsec, which occurs well before the peak of the $3 \rightarrow 2$ gain; this verifies that the lower-state kinetics are not sensitively dependent on the initial conditions of the states above $n=4$. The threshold for $3 \rightarrow 2$ gain is very sensitive to the initial $n=2$ population, requiring that the level be emptied to as little as 0.003 times the He-like ion density. Such a small ground-state population in Li-like Ne is achievable with OFI ionization based on tunneling ionization theory.[10] In computing the gain profiles, we have considered both Doppler and Stark line broadening.[11]

We focus on a particular fine-structure transition ($3d_{5/2} \rightarrow 2p_{3/2}$, $\lambda_x = 98$ Å) which has dominant gain compared to the other five fine-structure transitions. Since the gain associated with this transition can be

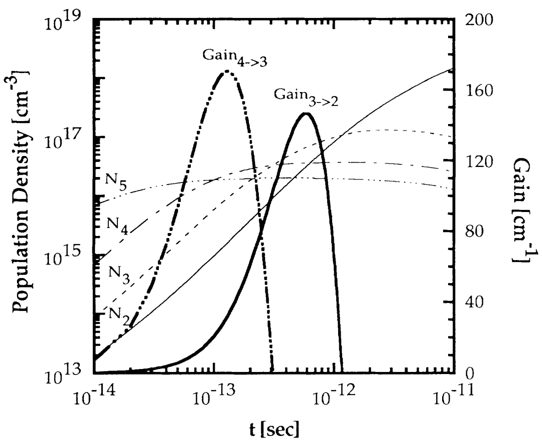

FIG. 1. The four lowest-level shell-averaged populations of Li-like Ne and indicated gain profiles for $n_e = 2.5\times10^{20}$ cm^{-3} and $T_e = 25$ eV.

large, particularly at low temperature and high density, it is necessary to consider the effects of gain saturation in this system. A specific (or per unit frequency) mean saturation intensity J_s is defined by equating the stimulated emission rate to *three* times the total exit rate from the (shell-averaged) upper state $\gamma_{\rm out}$, where $\gamma_{\rm out}$ includes all possible nonstimulated depletion processes of the upper state, when the lower state is *empty*. The factor of 3 arises because the stimulated rate refers to the $3d_{5/2}$ level which has only one-third of the $n=3$ population. We introduce an adjustable multiplier ($\alpha<3$) for the net stimulated emission rate at saturation, $\alpha\gamma_{\rm out}$, in order to model the stimulated emission rate with a *nonempty* lower-level population. With use of the Einstein formula for the net emission, we obtain

$$J_s = \alpha\gamma_{\rm out}\left[\frac{c^2}{2h\nu^3}A_{ul}\left(1-\frac{N_l' g_u}{N_u' g_l}\right)\right]^{-1}, \tag{1}$$

where the prime notation on the upper and lower fine-structure populations, N_u' and N_l', refers to their saturated values, g_u and g_l are degeneracy factors for the respective levels, A_{ul} is the spontaneous emission rate, and ν is the transition frequency. Since the population flow into the upper level is the same with or without stimulated emission, the flow out must be the same. Equating the outward population flow rates with and without stimulated emission, we have $3N_u\gamma_{\rm out} = 3N_u'\gamma_{\rm out} + N_u'\alpha\gamma_{\rm out}$, where the last term is the net stimulated emission contribution at saturation, and N_u is the upper-state population at maximum small-signal gain G. Defining $\beta = 1/(1+\alpha/3)$, we find that the saturated and unsaturated upper-level populations obey $N_u' = \beta N_u$. By choosing a physically relevant relation between N_l', N_l, N_u, N_u', and β, we can solve for β such that the gain when expressed in terms of primed populations is reduced by one-half compared to its small-signal value (unprimed). From the assumption that the upper and lower fine-structure levels are in statistical equilibrium, we require $N_l' = N_l + (1-\beta)N_u/2$, giving

$$\beta = \left[\frac{1}{2}\left(1+\frac{N_l g_u}{N_u g_l}\right)+\frac{1}{2}\frac{g_u}{g_l}\right]\Bigg/\left(1+\frac{1}{2}\frac{g_u}{g_l}\right). \tag{2}$$

In Eq. (2) we have not included the loss of lower-level population into the upper levels of Be-like Ne; thus, the associated gain is an underestimate since about 10% of the Li-like Ne ground state can be shown to rapidly fill the upper Be-like states by recombination. Finally, by solving the system of rate equations for the populations, we readily determine β from Eq. (2). We find that β is near unity, in strong contrast to the case of an empty lower state. From Fig. 1 the peak $4\to3$ gain occurs well before the $3\to2$ gain maximum, indicating the potential for enhanced $3\to2$ gain by virtue of an elevated $n=3$ population. Burnett and Enright[2] have surmised that stimulated radiative cascade may provide a factor-of-2 or -3 enhancement of the $3\to2$ gain. However, our analysis shows that the $n=3$ level is hardly affected by the $4\to3$ saturation due to small α, contributing minimally to the $3\to2$ gain.

Inserting α into Eq. (1) we obtain J_s and the saturated intensity $I_{\rm sat} = \Delta\nu J_s(2\pi^3/\ln2)^{1/2}$, where $\Delta\nu$ is the FWHM of the atomic line profile.[12] We require also the distance along the z axis at which the amplifying intensity reaches $I_{\rm sat}$. The saturation length $L_{\rm sat}$ is determined by equating J_s with the line mean (or Gaussian-line-profile-weighted) intensity $J(z) = \int I\,d\nu\,d\Omega/2\pi$. We demand that the resulting solutions for $L_{\rm sat}$ satisfy $a/L_{\rm sat} \le 0.05$ to distinguish our lasing system from a bright noise source. Finally, we may solve the line transfer equation for the intensity $I(z)$ in terms of $L_{\rm sat}$ and $I_{\rm sat}$:

$$I(z) = \begin{cases} I_{\rm sat} z/L_{\rm sat}, & z \ge L_{\rm sat}, \\ I_{\rm sat}(e^{Gz}-1)^{3/2}(GL_{\rm sat}e^{GL_{\rm sat}})^{1/2}/(Gze^{Gz})^{1/2}(e^{GL_{\rm sat}}-1)^{3/2}, & z \le L_{\rm sat}. \end{cases} \tag{3}$$

The effective distance of propagation of the driver laser pulse is limited by diffraction and is given by the confocal parameter,[13] $z = 4\pi a^2/\lambda\ln2$, where a is the half-intensity radius of the ionizing Gaussian laser pulse. However, z must not exceed the distance of required plasma ionization $z_I = 8I_{\rm req}\tau/n_e E_{\rm ion}$, where $E_{\rm ion}$ is the energy required to strip Ne to the He-like state (953.7 eV). This condition sets the maximum value of z at a few centimeters for $\tau\sim100$ fsec, $I_{\rm req}\sim10^{17}$ W/cm^2, and $n_e \sim 10^{20}$ cm^{-3}. Refraction from transverse ionization gradients may limit z to less than 1 mm (for $\lambda = 0.25$ μm), but focusing of the ionizing laser beam in a plasma waveguide should offset this effect.[2] The energy effi-

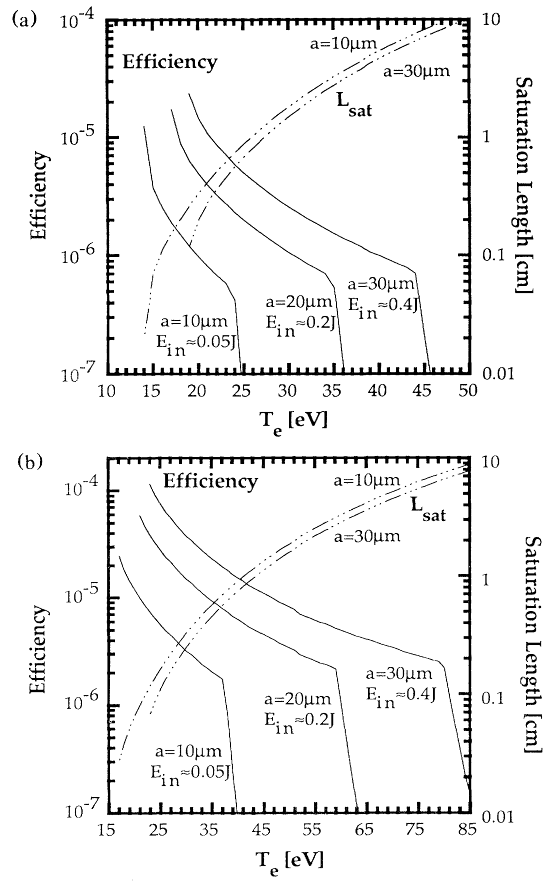

FIG. 2. Energy efficiency and saturation length $L_{\rm sat}$ in Li-like Ne vs temperature for several values of half-intensity radius a (corresponding to input energy $E_{\rm in}$). In (a) the electron density $n_e = 1.0\times10^{20}$ and for (b) $n_e = 2.5\times10^{20}$ cm^{-3}.

ciency is defined as the ratio of output energy $E_{\rm out} = I\Delta\tau\pi a^2$ to input energy $E_{\rm in} = I_{\rm req}\tau\pi a^2$, where $\Delta\tau$ is the temporal duration (FWHM) of the $3d_{5/2}\rightarrow 2p_{3/2}$ gain profile. In Figs. 2(a) and 2(b) we display the energy efficiency as a function of temperature for several values of a. An important feature of Figs. 2(a) and 2(b) is the strong dependence of efficiency on temperature which underscores the need to minimize electron heating. We have also plotted the efficiency versus electron density in Fig. 3 which shows a favorable trend when n_e is increased. However, this result is offset by the accompanying strong increase in parametric heating with n_e which we now consider.

There are several heating mechanisms which may plague the OFI ionization recombination x-ray laser scheme:[2] above threshold ionization (ATI), strong-field inverse bremsstrahlung, inelastic collisions, plasmon wake-field generation, and stimulated Compton or Raman scattering. Recent particle-in-cell (PIC) simulations of ATI heating with space-charge effects show that this source of heating is not serious if the plasma period

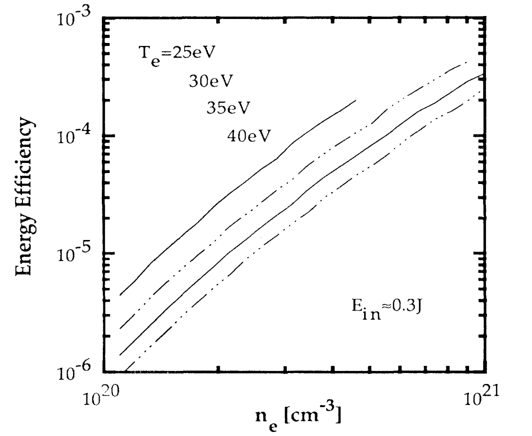

FIG. 3. Energy efficiency vs electron density n_e in Li-like Ne for half-intensity radius $a=25$ μm corresponding to an input energy $E_{\rm in}\approx 0.3J$.

is nonresonant with either the laser pulse length τ or the laser period $(1/\nu)$.[6] As an example, for $n_e \sim 10^{20}$ cm^{-3}, $\lambda \sim 0.25$ μm, $I_{\rm req} \sim 10^{17}$ W/cm^2, and $\tau \sim 100$ fsec, the electron heating from ATI is found to be on the order of 20 eV.[6] For these same conditions collisional heating is not important; additionally, inelastic collisions between electrons and He-like Ne ions occur too infrequently to be significant.[6] The role of parametric heating is conjectured to be potentially serious,[2,3] but a study of its effect in OFI ionization has not been carried out. Here we study parametric heating with the aid of a 2D PIC simulation, ZOHAR.[14]

Of the possible candidates for parametric heating, stimulated Raman backscatter commands primary attention. The associated linear growth rate γ scales as[15]

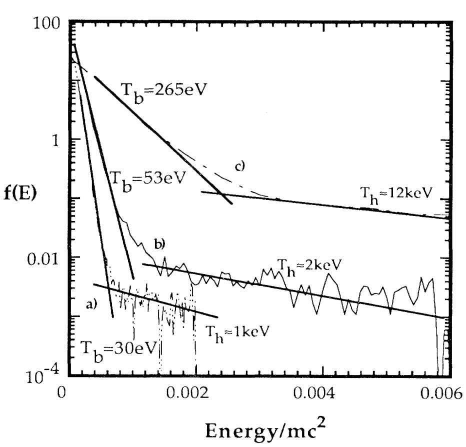

FIG. 4. Three electron distribution functions for three choices of electron density n_e: (a) 1.0×10^{20}, (b) 2.5×10^{20}, and (c) 5.0×10^{20} cm^{-3}. The heated background electron temperatures are denoted by T_b and the tail population temperatures by T_h.

$\gamma \approx (v_{osc}/2c)(\omega_{pe}\omega)^{1/2}$, where $v_{osc}=25.6 I_{req}^{1/2}\lambda$ is the electron quiver velocity (with v_{osc} in cm/sec and λ in μm), $\omega_{pe}=5.64\times10^4 n_e^{1/2}$ is the electron plasma frequency, and $\omega=2\pi\nu$. For $n_e \sim 10^{20}$ cm^{-3}, $\lambda \sim 0.25$ μm, and $I \sim 10^{17}$ W/cm^2, the growth time is on the order of 10 fsec, which is considerably less than available laser pulse lengths. We have started the simulation with an electron temperature of 25 eV to reflect supplemental heating from ATI and inverse bremsstrahlung. The electron distribution functions following the ionizing pulse are displayed in Fig. 4 for three values of electron density. For the moderate-density case 4(b), a low-temperature ($T_b \sim 53$ eV) background population is found along with a high-temperature ($T_h \sim 2$ keV), minority fractional population ($\leq 0.1\%$). This case represents the upper limit in plasma density for which plasma heating is tolerable under our adopted laser conditions; i.e., T_b must be sufficiently low to allow saturation ($z > L_{sat}$) in the system. For the lowest-density example 4(a), parametric heating contributes only 5 eV in additional heating. We conclude that laser pulses of 100-fsec duration at 0.25 μm and 10^{17} W/cm^2 require an electron density less than about 2.5×10^{20} cm^{-3} for the Li-like Ne scheme in order to yield efficiencies which are adequate ($>10^{-7}$) to distinguish the lasing transition from spontaneous noise. However, minimal parametric heating can occur if the laser-driver pulse length is only decreased to below ~ 75 fsec for $n_e = 5\times10^{20}$ cm^{-3}, giving efficiencies of $>10^{-5}$; cf Fig. 3. By further increasing n_e to 10^{21} cm^{-3} and decreasing the pulse length to 50 fsec, we have shown that efficiencies exceeding 10^{-4} are possible.

We have also found that extending the scheme to shorter wavelengths, e.g., Li-like Al at 52 Å, is not practical in the near term due to excessive parametric heating, e.g., $T_b \sim 1$ keV at $\tau = 50$ fsec, arising from the high-intensity requirement: $I_{req} \sim 10^{18}$ W/cm^2.

In summary, the prospect of high-intensity, short-pulse optical lasers should enable the demonstration of recombination x-ray lasing in the transient regime by OFI ionization. By further reducing the laser pulse length this scheme may possibly result in a viable tabletop x-ray laser.

We thank A. B. Langdon for use of his ZOHAR code and N. Bardsley, M. Dunning, C. Keane, W. Kruer, R. Lee, J. Lindl, R. London, S. Maxon, J. Nash, B. Penetrante, and M. Rosen for useful discussions. This work was performed under the auspices of the U.S. Department of Energy by Lawrence Livermore National Laboratory under Contract No. W-7405-ENG-48.

[1]For recent advances, see *Femtosecond to Nanosecond High-Intensity Lasers and Applications,* edited by E. M. Campbell (SPIE, Bellingham, 1990).

[2]N. H. Burnett and G. D. Enright, IEEE J. Quantum Electron. **26**, 1797 (1990).

[3]C. J. Keane, J. N. Bardsley, L. daSilva, N. Landen, and D. Matthews, in *Femtosecond to Nanosecond High-Intensity Lasers and Applications* (Ref. 1), pp. 190–195.

[4]M. D. Rosen *et al.*, Phys. Rev. Lett. **54**, 106 (1985); D. L. Matthews *et al., ibid.* **54**, 110 (1985); B. J. MacGowan *et al., ibid.* **65**, 420 (1990); R. C. Elton, *X-Ray Lasers* (Academic, San Diego, 1990).

[5]A. K. Dave and G. J. Pert, J. Phys. B **18**, 1027 (1985); N. H. Burnett and P. B. Corkum, J. Opt. Soc. Am. B **6**, 1195 (1989); D. C. Eder, Phys. Fluids B **2**, 3086 (1990).

[6]B. M. Penetrante and J. N. Bardsley, Phys. Rev. A **43**, 3100 (1991).

[7]R. M. More, J. Quant. Spectrosc. Radiat. Transfer **27**, 345 (1982).

[8]L. B. Golden, R. E. H. Clark, S. J. Goett, and D. H. Sampson, Astrophys. J. Suppl. **45**, 603 (1981); R. E. H. Clark, D. H. Sampson, and S. J. Goett, Astrophys. J. Suppl. **49**, 545 (1982).

[9]D. H. Sampson and H. Zhang, Astrophys. J. **335**, 516 (1988).

[10]M. V. Ammosov, N. V. Delone, and V. P. Krainov, Zh. Eksp. Teor. Fiz. **91**, 2008 (1986) [Sov. Phys. JETP **64**, 1191 (1986)].

[11]R. W. Lee, J. Quant. Spectrosc. Radiat. Transfer **40**, 561 (1988).

[12]R. A. London, Phys. Fluids **31**, 184 (1987).

[13]A. E. Siegman, *Lasers* (University Science Books, Mill Valley, CA, 1986).

[14]A. B. Langdon and B. F. Lasinski, in *Methods in Computational Physics,* edited by J. Killeen *et al.* (Academic, New York, 1976), Vol. 16.

[15]W. B. Kruer, *The Physics of Laser Plasma Interactions* (Addison-Wesley, New York, 1988).